

11

Noise in Semiconductor Devices

Alicja
Konczakowska
*Gdansk University
of Technology*

Bogdan M.
Wilamowski
Auburn University

11.1	Introduction	11-1
11.2	Sources of Noise in Semiconductor Devices	11-1
	Thermal Noise • Shot Noise • Generation-Recombination Noise • $1/f$ Noise • Noise $1/f^2$ • Burst Noise/RTS Noise Avalanche Noise	
11.3	Noise of BJTs, JFETs, and MOSFETs	11-6
	Noise of BJTs • Noise of JFETs • Noise of MOSFETs • Low Noise Circuits for Low Frequency Range	
	References.....	11-12

11.1 Introduction

Noise (a spontaneous fluctuation in current or in voltage) is generated in all semiconductor devices. The intensity of these fluctuations depends on device type, its manufacturing process, and operating conditions. The resulted noise, as a superposition of different noise sources, is defined as an inherent noise. The equivalent noise models (containing all noise sources) are created for a particular device: for example, bipolar transistor (BJT), junction field effect transistor (JFET), or metal oxide semiconductor field effect transistor (MOSFET).

The inherent noise of semiconductor devices is considered as an undesired effect and sometimes is referred to a useful signal. It is specially important for input (front-end) stages of electronic systems. However, the inherent noise can also be used for the quality assessment of semiconductor devices. Quite often it has been used as an important factor during the development of the production process of new semiconductor devices. Inherent noise is also used for the classification of semiconductor devices into groups with different quality and reliability.

The most important sources of noise are thermal noise, shot noise, generation-recombination noise, $1/f$ noise (flicker noise), $1/f^2$ noise, burst noise or random telegraph signal (RTS) noise, and avalanche noise. Detailed description of noise sources is presented in references [1–6].

11.2 Sources of Noise in Semiconductor Devices

11.2.1 Thermal Noise

Thermal noise is created by random motion of charge carriers due to the thermal excitation. This noise is sometimes known as the Johnson noise. In 1905, Einstein presented his theory of fluctuating movement of charges in thermal equilibrium. This theory was experimentally verified by Johnson in 1928. The thermal motion of carriers creates a fluctuating voltage on the terminals of each resistive element.

The average value of this voltage is zero, but the power on its terminals is not zero. The internal noise voltage source or current source is described by the Nyquist equation

$$\overline{v_{th}^2} = 4kTR\Delta f \quad \overline{i_{th}^2} = \frac{4kT\Delta f}{R} \quad (11.1)$$

where

k is the Boltzmann constant

T is the absolute temperature

$4kT$ is equal to $1.61 \cdot 10^{-20} \text{ V} \cdot \text{C}$ at room temperature

The thermal noise is proportional to the frequency bandwidth Δf . It can be represented by the voltage source in series with resistor R or by the current source in parallel to the resistor R . The maximum noise power can be delivered to the load when $R_L = R$. In this case, maximum noise power in the load is $kT\Delta f$. The noise power density, $dP_n/df = kT$, is independent of frequency. Thus, the thermal noise is the white noise. The RMS noise voltage and the RMS noise current are proportional to the square root of the frequency bandwidth Δf . The thermal noise is associated with every physical resistor in the circuit.

The spectral density function of the equivalent voltage and current thermal noise are given by

$$S_{thvR} = 4kTR \quad (11.2)$$

or

$$S_{thiG} = 4kTG \quad (11.3)$$

These noise spectral densities are constant up to 1 THz and they are proportional to temperature and to resistance of elements, and as such can be used to indirectly measure the following:

- The device temperature
- The base-spreading resistance of BJT
- The quality of contacts and connections

11.2.2 Shot Noise

Shot noise is associated with a discrete structure of electricity and the individual carrier injection through the pn junction. In each forward-biased junction, there is a potential barrier that can be overcome by the carriers with higher thermal energy. This is a random process and the noise current is given by

$$\overline{i_{sh}^2} = 2qI\Delta f \quad (11.4)$$

The noise spectral density function of the shot noise is temperature independent (white noise) and it is proportional to the junction current

$$S_{shi} = 2qI \quad (11.5)$$

where

q is the electron charge

I is the forward junction current

Shot noise is usually considered as a current source connected in parallel to the small signal junction resistance. The measurement of shot noise in modern nanoscale devices is relatively difficult since measured values of current are in the range of 10–100 fA.

Shot noise has to be proportional to the current and any deviation from this relation can be used to evaluate parasitic leaking resistances. It can be used for diagnosis of photodiodes, Zener diodes, avalanche diodes, and Schottky diodes.

11.2.3 Generation-Recombination Noise

Generation-recombination noise is caused by the fluctuation of number of carriers due to existence of the generation-recombination centers. Variation of number of carriers leads to changes of device conductance. This type of noise is a function of both temperature and biasing conditions. The spectral density function of the generation-recombination noise is described by

$$\frac{S_{g-r}(f)}{N^2} = \frac{(\overline{\Delta N})^2}{N^2} \cdot \frac{4\tau}{1 + (2\pi f \cdot \tau)^2} \quad (11.6)$$

where

$(\overline{\Delta N})^2$ is the variance of the number of carriers N

τ is the carrier lifetime

Spectral density is constant up to the frequency $f_{g-r} = 1/(2\pi\tau)$, and after that is decreasing proportionally to $1/f^2$.

In the case, when there are several types of generation-recombination centers with different carrier life time, the resultant noise spectrum will be a superposition of several distributions described by (11.6). Therefore, the spectral distribution of noise can be used to investigate various generation-recombination centers. This is an alternative method to deep-level transient spectroscopy (DLTS) to study generation-recombination processes in semiconductor devices.

11.2.4 $1/f$ Noise

$1/f$ noise is the dominant noise in the low frequency range and its spectral density function is proportional to $1/f$. This noise is present in all semiconductor devices under biasing. This noise is usually associated with material failures or with imperfection of a fabrication process. Most of research results conclude that this noise exists even for very low frequencies up to 10^{-6} Hz (frequency period of several weeks). This noise is sometimes used to model fluctuation of device parameters with time. There are two major models of $1/f$ noise:

- Surface model developed by McWhorter in 1957 [7]
- Bulk model developed by Hooge in 1969 [8]

The simplest way to obtain $1/f$ characteristics is to superpose many different spectra of generation-recombination noise, where free carriers are randomly trapped and released by centers with different life times. This was the basic concept behind the McWhorter model where it was assumed that

- In the silicon oxide near the silicon surface there are uniformly distributed trap centers.
- The probability of the carrier penetration to trap centers is decreasing exponentially with the distance from the surface.
- Time constants of trap centers increases with the distance from the surface.
- Trapping mechanisms by separate centers are independent.

The resulted noise spectral density function is given by

$$S_{1/f} \propto (\overline{\Delta N})^2 \int_{\tau_1}^{\tau_2} \frac{1}{\tau} \frac{4\tau}{1 + \omega\tau^2} \cdot d\tau = (\overline{\Delta N})^2 \cdot \frac{1}{f} \quad \text{for } \frac{1}{\tau_2} \ll \omega \ll \frac{1}{\tau_1} \quad (11.7)$$

The spectral density function is constant up to frequency $f_2 = 1/(2\pi\tau_2)$, then is proportional to $1/f$ between f_2 and $f_1 = 1/(2\pi\tau_1)$, from frequency f_1 is proportional to $1/f^2$. The McWhorter model is primarily used for MOSFET devices.

For BJT, the Hooge bulk model is more adequate. In this noise model, Hooge uses in the carrier transport two scattering mechanisms of carries: scattering on the silicon lattice and scattering on impurities. He assumed that only scattering on the crystal lattice is the source of the $1/f$ noise, while scattering on the impurities has no effect on noise level. All imperfections of the crystal lattice leads to large $1/f$ noise.

The noise spectral density function for the Hooge model is

$$S_{1/f} = \frac{\alpha_H \cdot I^\alpha}{f^\gamma \cdot N} \quad (11.8)$$

where

$\alpha_H = 2 \cdot 10^{-3}$ is the Hooge constant [8]

α and γ are material constants

N is the number of carriers

Later [9], Hooge proposed to use α_H as variable parameter, which in the case of silicon devices may vary from $5 \cdot 10^{-6}$ to $2 \cdot 10^{-3}$.

The $1/f$ noise is increasing with the reduction of device dimensions and as such is becoming a real problem for devices fabricated in nanoscale. The level of $1/f$ noise is often used as the measure of the quality of devices and its reliability. Devices fabricated with well-developed technologies usually have a much smaller level of $1/f$ noise. The $1/f$ noise (flicker noise) sometimes is considered to be responsible for the long-term device parameter fluctuation.

11.2.5 Noise $1/f^2$

Noise $1/f^2$ is a derivative of $1/f$ noise and it is observed mainly in metal interconnections of integrated circuits. It has become more evident for very narrow connections where there is a possibility of electromigration due to high current densities. In aluminum, the electromigration begins at current densities of $200 \mu\text{A}/\mu\text{m}^2$ and noise characteristics changes from $1/f^2$ to $1/f^\gamma$, where $\gamma > 2$. Also the noise level increases proportionally to the third power of the biasing current:

$$S_{1/f^2}(f) = \frac{C \cdot J^\beta}{f^\gamma \cdot T} \cdot \exp\left(\frac{-E_a}{k \cdot T}\right) \quad (11.9)$$

where

$\beta \geq 3, \gamma \geq 2$

C is the experimentally found constant

E_a is the activation energy of the electromigration

$k = 8.62 \cdot 10^{-5} \text{ eV/K}$ is the Boltzmann constant

The degeneration of the metallic layer is described by

$$v_d \propto J^n \exp\left(\frac{-E_a}{k \cdot T}\right) \quad (11.10)$$

Since Equations 11.9 and 11.10 have a similar character, the $1/f^2$ noise can be used as the measure of the quality of metal interconnections. This is a relatively fast and accurate method to estimate reliability of metal interconnections.

11.2.6 Burst Noise/RTS Noise

Burst noise is another type of noise at low frequencies. Recently, this noise was described as RTS noise. With given biasing condition of a device the magnitude of pulses is constant, but the switching time is random. The burst noise looks, on an oscilloscope, like a square wave with the constant magnitude, but with random pulse widths (see Figure 11.1). In some cases, the burst noise may have not two but several different levels.

Noise spectral density function of the RTS noise has a similar form like generation-recombination noise:

$$S_{RTS}(f) = C \frac{4 \cdot (\Delta I)^2}{1 + (2\pi f / f_{RTS})^2} \tag{11.11}$$

where

$$C = \frac{1}{(\bar{\tau}_l + \bar{\tau}_h) \cdot f_{RTS}^2}$$

$$f_{RTS} = \frac{1}{\bar{\tau}} = \frac{1}{\bar{\tau}_l} + \frac{1}{\bar{\tau}_h} = \frac{\bar{\tau}_l + \bar{\tau}_h}{\bar{\tau}_h \cdot \bar{\tau}_l}$$

RTS noise corner frequency, below this frequency spectrum of the

RTS noise is flat

T Observation time

$\bar{\tau}_l$ Average time of pulses at high level

$\bar{\tau}_h$ Average time of pulses at low level

AQ1
$$\bar{\tau}_l = \frac{1}{P} \sum_{i=1}^P \tau_{l,p}, \quad \bar{\tau}_h = \frac{1}{S} \sum_{j=1}^S \tau_{h,s}$$

The intensity of the RTS noise depends on the location of the trap center with the reference to the Fermi level. Only centers in the vicinity of Fermi levels are generating the RTS noise. These trapping centers, which are a source for RTS noise, are usually the result of silicon contamination with heavy metals or lattice structure imperfections.

In the SPICE program the burst noise is often approximated by

$$\overline{i_{RTS}^2} = K_B \frac{I^{A_B}}{1 + (f/f_{RTS})^2} \Delta f \tag{11.12}$$

where K_B , A_B , and f_{RTS} are experimentally chosen parameters, which usually vary from one device to another. Furthermore, a few different sources of the burst noise can exist in a single transistor. In such a case, each noise source should be modeled by separate Equation 11.11 with different parameters (usually different noise RTS corner frequency f_{RTS}).

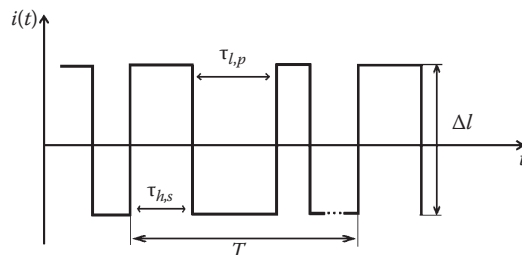


FIGURE 11.1 The RTS noise.

Kleinpenning [10] showed that RTS noise exists with devices with small number of carriers, where a single electron can be captured by a single trapping center. RTS noise is present in submicrometer MOS transistors and in BJTs with defected crystal lattice. It is present in modern SiGe transistors.

This noise has significant effect at low frequencies. It is a function of temperature, induced mechanical stress, and also radiation. In audio amplifiers, the burst noise sounds as random shots, which are similar to the sound associated with making popcorn. Obviously, BJTs with large burst noise must not be used in audio amplifiers and in other analog circuitry. The burst noise was often observed in epiplanar BJTs with large β coefficients. It is now assumed that devices fabricated with well-developed and established technologies do not generate the RTS noise. This is unfortunately not true for modern nanotransistors and devices fabricated with other than silicon materials.

11.2.7 Avalanche Noise

Avalanche noise in semiconductor devices is associated with reverse-biased junctions. For large reverse junction voltages the leakage current can be multiplied by the avalanche phenomenon. Carriers in the junctions gain energies in a high electrical field and then they collide with the crystal lattice. If the energy gained between collisions is large enough, then during collision another pair of carriers (electron and hole) can be generated. This way the revised biased current can be multiplied. This is a random process and obviously the noise source is associated with the avalanche carrier generation. The intensity of the avalanche noise is usually much larger than any other noise component. Fortunately, the avalanche noise exists only in the *pn* junction biased with a voltage close to the breakdown voltage. The avalanche phenomenon is often used to build the noise sources.

Noise spectral density function of the avalanche noise is frequency independent:

$$S_{av}(f) = \frac{2qI}{(2\pi f \cdot \tau)^2} \tag{11.13}$$

where I is an average value of the reverse biasing current.

An avalanche phenomenon is in most cases reversible. Therefore, semiconductor devices, where the avalanche breakdown took place, are regaining their low noise properties once devices are no longer working at avalanche region.

11.3 Noise of BJTs, JFETs, and MOSFETs

11.3.1 Noise of BJTs

In Figure 11.2, the equivalent diagram of BJT with noise sources is presented. These are as follows: thermal noise of base-spreading resistance r_b , shot noise and $1/f$ type noise of base bias current I_B , and

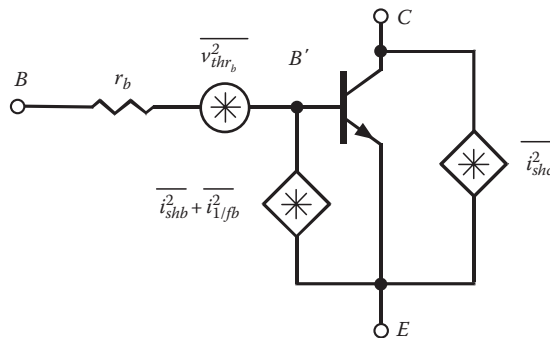


FIGURE 11.2 Equivalent diagram of BJT with noise sources.

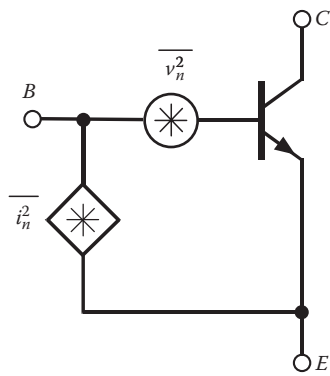


FIGURE 11.3 The $v_n^2 - i_n^2$ amplifier model of the bipolar transistor.

shot noise of collector current I_C . Spreading resistance is shown as external resistor r_b (noiseless resistor) between internal base B' and external base B.

The intensities (mean-square values) of noise sources are given by the following relations:

$$\overline{v_b^2} = 4kT r_b \cdot \Delta f \text{---thermal noise of base spreading resistance } r_b \quad (11.14)$$

$$\overline{i_{shb}^2} = 2q I_B \cdot \Delta f \text{---shot noise of base bias current } I_B \quad (11.15)$$

$$\overline{i_{1/fb}^2} = \frac{K_f \cdot I_B^\alpha \cdot \Delta f}{f^\gamma} \text{---flicker noise of base bias current } I_B \quad (11.16)$$

$$\overline{i_{shc}^2} = 2q I_C \cdot \Delta f \text{---shot noise of collector bias current } I_C \quad (11.17)$$

Coefficients α i γ in properly fabricated BJTs are close to 1. In silicon BJTs, the noise $1/f$ is caused by fluctuation of the recombination current in the depletion region of the base-emitter junction near the silicon surface. The *npn* transistors have usually higher levels of $1/f$ than *pnp* transistors.

Figure 11.3 shows the $v_n^2 - i_n^2$ amplifier model of the BJT with the equivalent input noise voltage and current $\overline{v_n^2}$ and $\overline{i_n^2}$, respectively.

The equivalent input noise voltage and current (mean-square values) can be expressed by [4]

$$\overline{v_n^2} = 4kT r_b \cdot \Delta f + \left(2q \cdot I_B \cdot \Delta f + \frac{K_f \cdot I_B^\alpha}{f^\gamma} \Delta f \right) \cdot r_b^2 + 2q I_C \cdot \Delta f \left(\frac{r_b}{\beta} + \frac{V_T}{I_C} \right)^2 \quad (11.18)$$

$$\overline{i_n^2} = 2q I_B \cdot \Delta f + \frac{K_f \cdot I_B^\alpha}{f^\gamma} \cdot \Delta f + \frac{2q I_C}{\beta^2} \cdot \Delta f \quad (11.19)$$

where β is the common-emitter current gain, $V_T = k \cdot T_0/q$, for $T_0 = 290$ K and $V_T = 25$ mV.

In practice, the intensities of these noise sources versus frequency f have to be taken into account, and of course the $1/f$ noise sources in low frequency range are the main ones. For this reason, the flicker noise corner frequency f_{cor} is one of the important parameter. The flicker noise corner frequency f_{cor} is understood as being the frequency for which the $1/f$ noise and the white noise (thermal, shot) are equal to each other (see Figure 11.4).

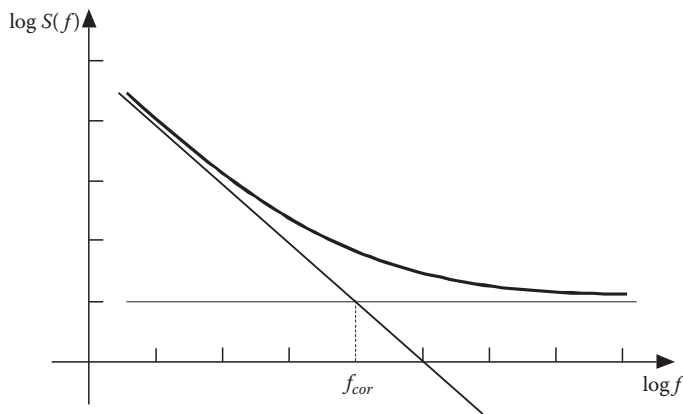


FIGURE 11.4 Noise power spectral density function $S(f)$ versus frequency f .

The shape of noise power spectral density function $S(f)$ as a function of frequency f , representing intensity of input noise voltage or current sources $\overline{v_n^2}/\Delta f, \overline{i_n^2}/\Delta f$, respectively, is the same. Function $S(f)$ should have -10 dB/decade slope in the low frequency range below flicker noise corner frequency f_{cor} . For the $f < f_{cor}$ the $1/f$ noise is the dominant component and for $f > f_{cor}$ the white (thermal and shot) noise is prevailing. The flicker noise corner frequency f_{cor} for $\overline{i_n^2}/\Delta f$ can be found from the relation [4]

$$f_{cor} = \frac{K_f}{2q(1+1/\beta)} \tag{11.20}$$

where parameters K_f and β are measured experimentally.

For BJTs, the f_{cor} is in the range from tenth of Hz to several kHz. The value of the flicker noise corner frequency can be evaluated separately for both equivalent input noise sources, for equivalent input noise voltage, and equivalent input noise current. The values of f_{cor} are not the same.

For evaluating a noise behavior of BJTs in a high and a very high frequency range the noise factor F can be applied. The noise factor F is given by the relation

$$F = \frac{\overline{v_{ni}^2}}{4kTR_S\Delta f} \tag{11.21}$$

where $\overline{v_{ni}^2}$ is the mean-square equivalent noise input voltage for the CE or the CB configuration of BJT, R_S is the noise source resistance [4].

One way to reduce the thermal noise level of the base spreading resistance, r_b , is the connection of several (N) BJTs in parallel and to assure that the total current of all transistors is the same as for one transistor. By this way, the level of shot noise stays on the same level and the thermal noise is reduced to r_b/N .

11.3.2 Noise of JFETs

In Figure 11.5, the equivalent diagram of JFET with attached noise sources is presented. These are as follows: thermal noise of drain current I_D , $1/f$ noise of drain current I_D , and shot noise of gate current I_G . At the normal operating conditions, the gate-source junction is reverse biased and the shot noise of gate current, I_G , can be neglected.

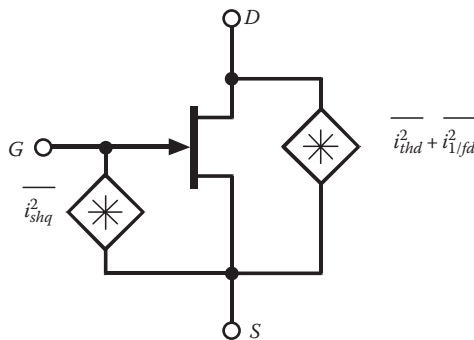
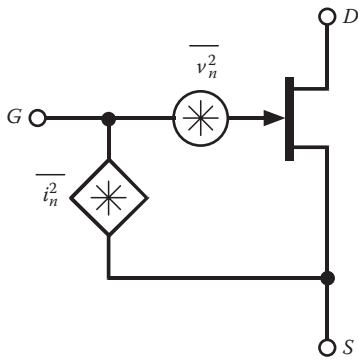


FIGURE 11.5 Equivalent diagram of JFET with noise sources.



The intensities (mean-square values) of noise sources are given by the following relations:

$$\overline{i_{shg}^2} = 2qI_G \cdot \Delta f \text{—shot noise of gate current } I_G \quad (11.22)$$

$$\overline{i_{thd}^2} = 4kT \left(\frac{2g_m}{3} \right) \cdot \Delta f \text{—thermal noise of drain current } I_D \quad (11.23)$$

$$\overline{i_{1/fd}^2} = \frac{K_f \cdot I_D^\alpha}{f^\gamma} \cdot \Delta f \text{—flicker noise of drain current } I_D \quad (11.24)$$

FIGURE 11.6 The $v_n^2 - i_n^2$ amplifier model of the JFET.

Coefficients α i γ in properly fabricated JFETs are close to 1.

Figure 11.6 shows the $v_n^2 - i_n^2$ amplifier model of the JFET with the equivalent input noise voltage and current $\overline{v_n^2}$ and $\overline{i_n^2}$, respectively.

The equivalent input noise voltage and current (mean-square values) can be expressed by [4]

$$\overline{v_n^2} = \frac{\overline{i_{thd}^2} + \overline{i_{1/fd}^2}}{g_m^2} = 4kT \left(\frac{2}{3g_m} \right) \cdot \Delta f + \frac{K_f \cdot I_D^\alpha}{g_m^2 \cdot f^\gamma} \cdot \Delta f = \frac{4kT \cdot \Delta f}{3\sqrt{\beta} \cdot I_D} + \frac{K_f \cdot \Delta f}{4\beta \cdot f} \quad (11.25)$$

$$\overline{i_n^2} = \overline{i_{shg}^2} = 2qI_G \cdot \Delta f \quad (11.26)$$

where β is the transconductance coefficient.

As for BJTs, in the low frequency range, the flicker noise corner frequency f_{cor} is one of the important parameter. The frequency f_{cor} can be evaluated only for the power spectral density function $S(f)$ representing the intensity of input noise voltage $\overline{v_n^2}/\Delta f$, because the equivalent input noise current does not include the $1/f$ noise. For JFETs, the flicker noise frequency f_{cor} is understood as being the frequency for which the $1/f$ noise and thermal noise of $\overline{v_n^2}/\Delta f$ are equal to each other (see Figure 11.4).

Noise power spectral density function $S(f)$ as function of frequency f (representing intensity of input noise voltage source) should have -10 dB/decade slope in the low frequency range below flicker noise corner frequency f_{cor} . For the $f < f_{cor}$, the $1/f$ noise of drain current is the dominant component; and for $f > f_{cor}$ the thermal noise of drain current is prevailing.

The flicker noise corner frequency f_{cor} for $\overline{v_n^2}/\Delta f$ can be calculated from the relation

$$f_{cor} = \frac{3 \cdot K_f}{16 \cdot kT} \sqrt{\frac{I_D}{\beta}} \quad (11.27)$$

The typical flicker noise corner frequency f_{cor} for JFETs is in the range of several kHz.

For high and very high frequency, the noise factor F for JFETs can be calculated using relation (11.21), where $\overline{v_n^2}$ is the mean-square equivalent noise input voltage for the CS or the CG configuration of JFET, and R_s is the noise source resistance [4].

11.3.3 Noise of MOSFETs

In Figure 11.7, the equivalent diagram of MOSFET with attached noise sources is presented. These are as follows: thermal noise of drain current I_D and $1/f$ noise of drain current I_D .

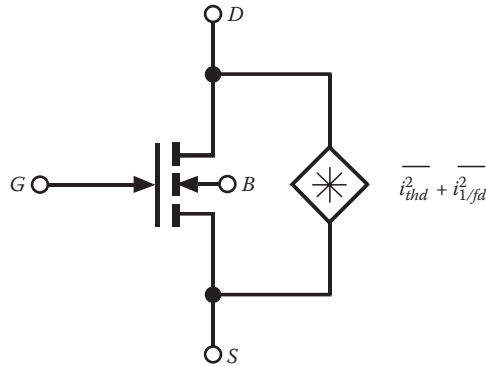


FIGURE 11.7 Equivalent diagram of MOSFET with noise sources.

The intensities (mean-square values) of noise sources are given by the following relations:

$$\overline{i_{thd}^2} = 4kT \left(\frac{2g_m}{3} \right) \cdot \Delta f \text{—thermal noise of drain current } I_D \tag{11.28}$$

$$\overline{i_{1/fd}^2} = \frac{K_f \cdot I_D^\alpha}{L^2 C_{ox} f^\gamma} \cdot \Delta f \text{—flicker noise of drain current } I_D \tag{11.29}$$

where

- L is the channel length
- C_{ox} is the gate oxide capacitance per unit area
- Coefficients α i γ in properly fabricated MOSFETs are close to 1.

Figure 11.8 shows the $v_n^2 - i_n^2$ amplifier model of the MOSFET with the equivalent input noise voltage and current $\overline{v_n^2}$ and $\overline{i_n^2}$, respectively.

The equivalent input noise voltage and current (mean-square values) can be expressed by [4]

$$\overline{v_n^2} = \frac{\overline{i_{thd}^2} + \overline{i_{1/fd}^2}}{g_m^2} = \frac{4kT \cdot \Delta f}{3\sqrt{K} \cdot I_D} + \frac{K_f \cdot \Delta f}{4KL^2 C_{ox} \cdot f^\gamma} \tag{11.30}$$

$$\overline{i_n^2} = 0 \tag{11.31}$$

where K is the transconductance coefficient.

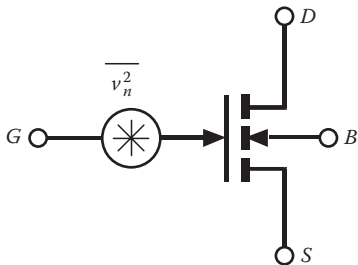


FIGURE 11.8 The $v_n^2 - i_n^2$ amplifier model of the MOSFET.

From the noise power spectral density function $S(f)$ versus frequency f (representing intensity of input noise voltage source), the flicker noise corner frequency f_{cor} can be found (see Figure 11.4).

This noise corner frequency f_{cor} for $\overline{v_n^2} / \Delta f$ can be evaluated from the relation

$$f_{cor} = \frac{3 \cdot K_f}{16 \cdot kTL^2 C_{ox}} \cdot \sqrt{\frac{I_D}{K}} \tag{11.32}$$

For the $f < f_{cor}$, the $1/f$ noise of drain current is the dominant component; and for $f > f_{cor}$, the thermal noise of drain current is prevailing.

The typical values of f_{cor} in MOSFETs could be even larger than 10 MHz. The noise level at very high frequencies is very low.

11.3.4 Low Noise Circuits for Low Frequency Range

There are special semiconductor devices named “noiseless” that have very low levels of noise, especially in the low frequency range. These are transistors (bipolar and unipolar), transistor pairs, specially matched transistors, and amplifiers. For these devices, the equivalent input noise voltage source or the equivalent input noise current source (see Figure 11.3 for BJTs, Figure 11.6 for JFETs, Figure 11.8 for MOSFETs) at low frequency is given in technical data by manufacturers. Typically, this information is given for 1 kHz (sometimes for 10 Hz) at the given value of the device current. For these devices, the $1/f$ noise intensity and flicker noise corner frequency are important.

For low noise system, the input (front-end) stages are very important. For small source resistances, the BJTs are the preferred devices for these stages, and typically they have about 10 times lower level of equivalent input noise voltage than JFETs. In the selection of the BJT, the large value of the current gain β and the small value of the base spreading resistance r_b is important. For example, BJTs *nnp* 2SD786 i *pnp* 2SB737 of Japanese company ROHM have $\beta = 400$ and $r_b = 4 \Omega$. Transistors MAT-2 from Analog Devices (monolithic transistor pair) have $\beta = 500$ and r_b below 1Ω . Noise parameters of transistors MAT 02E are as follows: intensity of equivalent input noise voltage source at collector current of 1 mA at frequency 10 Hz is equal to $1.6/2 \text{ nV}/\sqrt{\text{Hz}}$, at frequency 100 Hz is $0.9/1 \text{ nV}/\sqrt{\text{Hz}}$, and at frequency 1–100 kHz is $0.85/1 \text{ nV}/\sqrt{\text{Hz}}$.

For high source resistances, the JFETs are the preferred choice. It is important that JFET transistors have large transconductance g_m and small gate capacitance. For transistors 2N5515 made by INTENSIL, the intensity of equivalent input noise current source at 10 Hz and 1.6 mA is smaller than $1 \text{ fA}/\sqrt{\text{Hz}}$, and is the same up to 10 kHz. Whereas, the intensity of equivalent input noise voltage source at drain current of $600 \mu\text{A}$ is $10 \text{ nV}/\sqrt{\text{Hz}}$. This transistor has $f_{cor} = 10 \text{ kHz}$ at drain current of $600 \mu\text{A}$; it means that at 10 kHz the intensity of $1/f$ noise is equal to intensity of white noise.

For low frequencies, MOSFETs should not be used because of the high level of $1/f$ noise.

There are also special operational amplifiers for low noise applications. One such amplifier is manufactured by Precision Monolithics Inc. and it has the intensity of equivalent input noise voltage source in the range $3.5/5.5 \text{ nV}/\sqrt{\text{Hz}}$ at 10 Hz and $3/3.8 \text{ nV}/\sqrt{\text{Hz}}$ at 1 kHz. Whereas, the intensity of equivalent current noise source is $1.7/4 \text{ pA}/\sqrt{\text{Hz}}$ at 10 Hz, and $0.4/0.6 \text{ pV}/\sqrt{\text{Hz}}$ at 1 kHz. This low noise OPAMP has very small flicker noise corner frequency, which is equal to 2.7 Hz for equivalent input noise voltage source and 140 Hz for equivalent input noise current source. This amplifier is specially suited for small source resistances ($R_s < 1 \text{ k}\Omega$). For input resistances larger than $1 \text{ k}\Omega$, better noise property have amplifiers OP-07 i OP-08. For very large input resistances, the better choice is OPA-128, which has intensity of equivalent input noise voltage source equal to $27 \text{ nV}/\sqrt{\text{Hz}}$ at 1 kHz, and intensity of equivalent input noise current source is $0.12 \text{ fA}/\sqrt{\text{Hz}}$ in the frequency range from 0.1 Hz to 20 kHz. The low noise amplifiers AD 797 from Analog Devices has the intensity of equivalent input noise voltage source equal to $1.7 \text{ nV}/\sqrt{\text{Hz}}$ at 10 Hz and $0.9 \text{ nV}/\sqrt{\text{Hz}}$ at 1 kHz. Similar properties have low noise amplifiers LT 1028/LT 1128 from LINEAR TECHNOLOGY. They have the intensity of equivalent input noise voltage source equal to $1 \text{ nV}/\sqrt{\text{Hz}}$ at 10 Hz and $1.1 \text{ nV}/\sqrt{\text{Hz}}$ at 1 kHz. The flicker noise corner frequency f_{cor} is very low and it is equal to 3.5 Hz.

A special low noise amplifier for sources with large resistances is TLC 2201. It has, at 100 Hz, the intensity of equivalent input noise voltage source of $10 \text{ nV}/\sqrt{\text{Hz}}$, and the intensity of equivalent input noise current source of $0.6 \text{ fA}/\sqrt{\text{Hz}}$.

In practical applications, for very low noise circuits usually in the first stage of the system low noise transistor is applied and then at the next stages low noise amplifiers are used. Special care should also be taken for proper design of power supplies.

References

1. Ambrozy A. *Electronic Noise*. Akademiai Kiadó, Budapest, Hungary, 1982.
2. Konczakowska A. *Szumy z zakresu małych częstotliwości*. Akademicka Oficyna Wydawnicza EXIT, Warszawa, Poland, 2006.
3. Lukyanchikova N. *Noise Research in Semiconductor Devices*. B. K. Jones (Ed.), Gordon and Breach Science Publisher, Amsterdam, the Netherlands, 1996.
4. Marshall Leach W. Jr. *Fundamentals of Low-Noise Electronics*. Georgia Institute of Technology, School of Electrical and Computer Engineering, Atlanta, GA, 1999–2008.
5. Motchenbacher C. D., Fitchen F. C. *Low-Noise Electronic System Design*. A Wiley-Interscience Publication, John Wiley & Sons, Inc., New York, 1993.
6. Van der Ziel A. *Noise in Solid State Devices and Circuits*. John Wiley & Sons, New York, 1986.
7. McWhorter A. L. $1/f$ noise and germanium surface prosperities. In *Semiconductor Surface Physics*. R. H. Kingdon (Ed.), University of Pennsylvania Press, Philadelphia, PA, 1957, pp. 207–228.
8. Hooge F. N. $1/f$ noise is no surface effect. *Physics Letters*, 29A (3), 1969, 139–140.
9. Hooge F. N. The relation between $1/f$ noise and number of electrons. *Physica B*, 162, 1990, 334–352.
10. Kleinpenning T. G. M. On $1/f$ noise and random telegraph noise in very small electronic devices. *Physica B*, 164, 1990, 331–334.